The HER in alkaline media on Pt-modified three-dimensional Ni cathodes

Stefania Fiameni[a], Isaac Herraiz-Cardona[b], Marco Musiani[a*], Valentín-Pérez-Herranz[b], Lourdes Vázquez-Gómez[a], Enrico Verlato[a]

[a]IENI CNR, Corso Stati Uniti 4, 35127 Padova, Italy
[b]Ingeniería Electroquímica y Corrosión (IEC), Departamento de Ingeniería Química y Nuclear, Universitat Politècnica de València, Camino de Vera s/n, 46022 Valencia, Spain

Abstract

Electrodeposited porous Ni layers and commercial Ni foams were submitted to spontaneous deposition of Pt, achieved by immersing the Ni substrates in H_2PtCl_6 solutions, at open circuit, to produce Pt-modified 3D Ni electrodes. When using Ni foams, the immersion was prolonged until the whole amount of H_2PtCl_6 in the solution had reacted. Such an approach, which granted an easy control of the Pt loading, could not be used for Ni electrodeposits, since they underwent significant corrosion. The true Pt surface area was determined by measuring, for each electrode, the hydrogen desorption charge according to methods described in the literature. The ratios between Pt surface area and Pt loading were higher for Ni foam electrodes than for porous Ni electrodeposits. Both kinds of Pt-modified
Ni electrodes were used as cathodes for hydrogen evolution in 1 M KOH. Cathodes with Pt loading below 0.5 mg cm^{-2} (referred to geometric surface area) evolved hydrogen at
-100 mA cm^{-2} with a -75 mV overpotential. The better activity of foam electrodes as compared to electrodeposits, especially at low Pt loading, was mainly due to their higher Pt surface area per unit Pt mass.

Keywords: Electrocatalysis Foam electrodes; Galvanic displacement; HER; Porous electrodes; Spontaneous deposition

1. Introduction

The hydrogen evolution reaction (HER) is the cathodic process in many important electrochemical technologies, mainly alkaline water electrolysis and chlor-alkali production. The former is a key stage in the sequence of technologies necessary to sustain a hydrogen economy [1,2]. Although the HER is a kinetically facile reaction, less demanding than oxygen evolution [3], its contribution to the cell voltage necessary to drive water electrolysis cannot be neglected. Therefore, research on cathode materials actively continues in several directions (for a recent review, see [4]). As for all electrocatalytic processes, the optimum electrode materials for HER must combine strong intrinsic catalytic activity, large surface area, stability of performance and low cost. As these requirements are never fulfilled simultaneously by a simple material, composite electrodes consisting of highly catalytic noble metals supported by non-noble substrates were already developed some decades ago [5,6]. Recent work along this line further explored the use of porous layers of Ni, modified with either Ru or Ir [7,8], as cathodes for HER in basic media. These Ni porous layers, obtained by electrodeposition from $NiCl_2$, NH_4Cl solutions [9,10], were mechanically robust, and thus were not damaged under gas evolution conditions, had large surface areas, roughly proportional to their thickness [11], and spontaneously reacted with solutions of noble metal complex ions, becoming coated by Ru or Ir micro-crystals [7]. Clearly, both the intrinsic properties of the noble metal and its electro- chemically active surface area determine the activity of composite electrodes. The work described in the present paper was aimed at extending the same approach to the activation of Ni, in two directions: (i) the spontaneous deposition of Pt, the most active catalytic material for HER [3], and (ii) the use of commercial Ni foams, as large surface area substrates, in addition to electrodeposited porous layers. Major differences between these two kinds of substrates are their pore dimensions (of the order of hundreds of nanometers to a few micrometers for the former, and of hundreds of micrometers for the latter) and their thickness (around 20 mm for the electrodeposits, and ca. 1.70 mm for the foams). Ni foams were previously used by several groups in the preparation of electrocatalysts for various electrochemical processes [12-23].

An especially simple method for the deposition of noble metals is spontaneous deposition, also called galvanic displacement, immersion plating or displacement plating, which takes place at open circuit by

immersion of a less noble metal substrate in a solution containing ions of a more noble metal. For example, neglecting the actual complex nature of the ions present in solution, the Pt-Ni exchange may be schematically written:

$$2Ni(0) + Pt^{4+}_{sol} \rightarrow 2Ni^{2+}_{sol} + Pt(0) \qquad (1)$$

Several research groups have investigated spontaneous deposition as a method for the preparation of catalysts and especially electrocatalysts [5-8, 24-36] because noble metal clusters or monolayers formed on non-noble substrates may greatly enhance their catalytic activity. Occurring at open circuit, the spontaneous deposition is likely to take place on the whole substrate surface, including the inner surface of the pores, unlike electrodeposition which, when carried out onto porous electrodes, may be quite sensitive to inhomogeneous current distribution.

A key issue in the preparation of modified electrode is the control of the noble metal loading, which must be kept quite low in order to optimize the mass activity of the catalysts, and therefore their cost. A priori, the easiest way to achieve such a control is using, in the spontaneous deposition reactions, small volumes of diluted solutions of noble metal ions and immersion times long enough to allow all the noble metal to deposit. Henceforth, this method will be called “exhaustive spontaneous deposition”. An advantage of this approach is that no noble metal is wasted. A possible draw- back is the fact that, for kinetically fast metal exchange reactions, and diluted noble metal ion solutions, the noble metal deposition may occur under (partial) diffusion control; if so, the solution inside narrow pores may become depleted, and the resulting noble metal deposits may be unevenly distributed.

In the following, the preparation of Pt-modified Ni porous layers and Ni foams will be described. Data on the morphology and the true surface area of the Pt deposits will be presented. Finally, the activity of Pt-modified Ni electrodes as cathodes for the HER in basic solutions will be described.

2. Experimental

2.1. Equipment and materials.

Porous Ni layers were deposited onto Ni disc electrodes (0.34 cm^2 geometric area). Prior to use, these electrodes were polished with emery paper 1000, rinsed with water and dried in air. Ni electrodeposition was performed, in a cell consisting of a main central cylindrical compartment, where the Ni disc electrode was positioned, connected through glass frits to two lateral compartments where two Ni wire counterelectrodes (overall area 2 cm^2) were placed. In order to remove hydrogen bubbles formed in a side reaction, the working electrode was rotated at 2500 revolutions per minute.

The Ni foam electrodes were 0.5 cm x 0.5 cm x 0.17 cm parallelepipeds (volume 0.0425 cm^3) produced from 0.17 cm thick INCOFOAM™ sheets, with 50 pores per linear inch. Before use, the Ni foam was successively washed with acetone and dichloromethane, dried in an air stream and then etched in an acid solution (typically 2 M HCl at 60 ^{o}C for 15 min).

A Pt disc electrode (0.0016 cm^2 geometric area), carefully polished with alumina down to 0.05 mm, was used for comparison, in voltammetric experiments aimed at measuring the true surface area of Pt deposits.

A two-compartment cell was used in voltammetric and EIS experiments, and for recording pseudo-steady-state currentepotential curves. The working electrode and a Pt wire used as counterelectrode were inserted in the main compartment, and an Hg/HgO/1 M KOH electrode, used as reference, was placed in the lateral compartment connected to the main one through a Luggin capillary. Hence-forth, all potentials are referred to Hg/HgO/1 M KOH. When a disc electrode bearing a Ni porous layer was used as working electrode, it was positioned in such a way that the electrode/electrolyte interface was on a vertical plane, so as to allow, when necessary, the free release of the hydrogen bubbles produced. Foam electrodes were placed with the 0.5 cm x 0.5 cm faces on a vertical plane. The current densities measured with porous electrodeposits or foam electrodes are referred to either the true surface area of the Ni substrate, and denoted *j*, or to the working electrode geometric area (0.34 cm^2 for disc electrodes and 0.755 cm^2 for foam electrodes), and denoted

j_{geo}. For polished disc electrodes j and j_{geo} were assumed to coincide.

The electrochemical equipment consisted of an EG&G Princeton Applied Research Potentiostat/Galvanostat 273A and of an Autolab PGSTAT 100. The latter was used for EIS experiments. SEM analyses were performed with a Fei- Esem FEI Quanta 200 FEG instrument, equipped with a field emission gun, operating in high vacuum condition at an accelerating voltage variable from 5 to 30 keV, depending on the observation needs. EDS analyses were obtained by using an EDAX Genesis energy-dispersive X-ray spectrometer at an accelerating voltage of 25 keV. The Pt ion concentration in the solutions used for spontaneous deposition was assessed with a Thermo Elemental - X7 Quadrupole ICP-MS.

2.2. Procedures.

Porous Ni layers were galvanostatically deposited from 0.2 M $NiCl_2$, 2 M NH_4Cl aqueous solutions, pH 4.5, kept at 25 ^{o}C [9e11], typically at a current density of -1.0 A cm^{-2}. The layer thickness was controlled through the deposition charge which was fixed, in all experiments, at 60 C cm^{-2}. Such a charge, taking into account the current efficiency of Ni deposition, and neglecting the pores volume, corresponded to a Ni layer thickness around 20 mm [11]. The true surface area of the Ni electrodeposits was measured as described in previous papers [7,33,36] and reproducibly found to be 6.8 ± 0.4 cm^2 (corresponding to a surface roughness factor ca. 20). The true surface area of etched Ni foams was similarly measured; electrodes with a 0.0425 cm^3 volume had surface areas of 12 ± 0.5 cm^2 [23], i.e. their surface roughness factor was ca. 16.

The spontaneous deposition of Pt was carried out by immersing the porous Ni layers or the Ni foam electrodes, at open circuit in acid H_2PtCl_6 solutions, kept at 25 ^{o}C by means of a thermostat, and thoroughly purged with an N_2 flow. When using Ni foams, the H_2PtCl_6 concentration was in the range 5 x 10^{-5} Me1 x 10^{-3} M and the immersion lasted long enough to allow exhaustive Pt deposition, i.e. to allow all H_2PtCl_6 to react with Ni and deposit as metal. Thus the H_2PtCl_6 concentration and the solution volume were the sole experimental variables, and the Pt loading could be assumed to coincide with the total Pt amount initially present in the

solution. As previous experience had shown that porous layers were corroded more extensively than Ni foams during spontaneous deposition [23,33,36], milder deposition conditions, i.e. larger volumes of less acid (pH 2 instead of 1) and less concentrated H_2PtCl_6 solutions, were used for the porous layers than for the foams. The duration of the immersion (t_{SD}) was generally not long enough to cause exhaustive Pt deposition. For these samples the Pt loading was estimated by measuring, with ICP- MS, the decrease in the H_2PtCl_6 concentration caused by the deposition [23].

Pristine and Pt-modified Ni electrodes were submitted, at first, to cyclic voltammetry in 1 M KOH aqueous solutions, in a potential range encompassing both the $Ni(OH)_2/NiOOH$ inter-conversion [37] and hydrogen adsorption/desorption [38e41], with the aim to estimate the surface areas of both Ni substrates and Pt deposits. Five cycles were recorded in succession, at 50 mV s^{-1}. The cyclic voltammograms shown below are always the last of each series, corresponding to a stabilized behavior. Then, the hydrogen evolution reaction was studied in the same electrolyte, by recording pseudo- steady-state current-potential curves at 1 mV s^{-1}. Tafel plots were obtained from these curves, after correction of the R_e x i drop; the value of the electrolyte resistance R_e was determined, at each potential, as the high frequency limit of the impedance measured with the same electrode, electrolyte and cell geometry. In EIS experiments, the frequency range 100 mHz-100 kHz was covered with 8 points per decade. The amplitude of the modulated potential was 10 mV.

3. Results and discussion

3.1. Spontaneous deposition of Pt; SEM-EDS characterization

Preliminary tests were run to establish the minimum immersion duration (t_{SD}^{o}) that allowed exhaustive deposition of Pt onto Ni foam substrates, for different H_2PtCl_6 concentrations. The deposition was assumed to be complete when the H_2PtCl_6 concentration (assessed by ICP-MS) had decreased to less than 1% of its initial value. For foam substrates, for example, ca.

7 h were necessary to achieve exhaustive deposition of Pt from 5 mL of a 10^{-3} M solution; for $[H_2PtCl_6] \leq 4 \times 10^{-4}$ M, 5 h or less were needed. Unless these immersion durations were very largely exceeded, Ni foam did not undergo visible corrosion upon prolonging the immersion beyond t_{SD}^{o}. Working with electrodeposited porous Ni layers was trickier, due to their lower resistance to corrosion. The SEM images in Fig.1 show two samples immersion plated in 30 mL of 6.8 M x 10^{-5} M H_2PtCl_6 solution for 8 h (A) and in 30 mL of 1.37 x 10^{-4} M H_2PtCl_6 solution for 16 h (B), respectively. The usual dendritic structure of the porous Ni deposit was retained by sample A (compare SEM images in [7,11]), for which t_{SD} was markedly lower than t_{SD}^{o}. Instead, the structure of sample B was profoundly altered: some dendrites, extensively coated by Pt were still visible, but many others had disappeared. One may speculate that the partial processes of reaction (1), $Pt^{4þ}$ reduction and Ni oxidation, had occurred at different positions, in a localized way. Some Ni dendrites behaved as cathodes, becoming coated by Pt, other dendrites behaved as anodes and underwent more or less complete corrosion. These and similar experiments carried out during this investigation showed that exhaustive deposition was not a viable method for modifying Ni electrodeposits with noble metal nuclei. Therefore, Pt-modified Ni electrode- posits were prepared with immersion durations significantly lower than t_{SD}^{o} and their Pt loading was assessed by ICP-MS analyses.

Fig. 2A shows the same sample as in Fig. 1A, with a larger magnification. Pt deposits were evident, especially on top of the dendrites. EDS analyses were performed both on extended areas, typically 60 mm x 50 mm, and on top of individual dendrites. Although such analyses were devoid of a rigorous quantitative character, they clearly showed that the Pt/Ni

ratio was significantly higher on the protruding parts of the deposits than on the average (extended areas). This result suggests that deposition of Pt was inhomogeneous, most probably because of slow mass transport toward recessed areas inside the pores. Fig. 2B shows the Pt deposit formed by exhaustive deposition onto a Ni foam sample. Needle-like Pt crystals homogeneously covered the Ni substrate. EDS analyses performed by selectively sampling the walls of either inner or outer cells of the foam showed comparable Pt/Ni ratios, suggesting that mass transport limitations were unimportant for the foam samples with pore dimensions ca. 100 times larger than those of electro- deposited porous layers.

3.2. Cyclic voltammetries of Pt and Pt-modified Ni electrodes in 1 M KOH

Fig. 3 shows a series of cyclic voltammograms recorded with a Pt disc electrode in 1 M KOH, at 50 mV s^{-1}, with variable anodic limits (E_A). The overall pattern agrees with those reported by other authors [40,41]. As E_A became progressively more positive, a cathodic peak ascribed to the reduction of Pt surface oxides became increasingly evident, during the reverse scan. Its size increased and its position shifted to more negative potential values as E_A increased. Peaks corresponding to the adsorption of hydrogen and to its desorption were visible, during the cathodic and anodic scans, respectively, in the range -0.5 to -0.85 V. These peaks were much less sensitive to E_A than the reduction of Pt oxides. Although in basic solutions they were less well separated from hydrogen evolution than in acid media [38e41], the charge associated to H desorption could be measured in a potential range where neither Pt oxidation nor hydrogen evolution had significant effect. Therefore that desorption charge could be safely assumed to be proportional to the Pt surface area. An average desorption charge of 190 mC cm^{-2} was measured in several experiments carried out in 1 M KOH, in good agreement with data in the literature reporting a desorption charge of 210 mC cm^{-2}, in acid media [38].

Fig. 4 highlights the hydrogen adsorption/desorption region of the voltammograms recorded with Ni foam electrodes modified by exhaustive deposition of Pt, at two H_2PtCl_6 concentrations (the whole voltammograms are shown in the inset). For each concentration, two immersion times are reported, one just above t_{SD}^{o} (t_{SD}^{o} was shorter

than 5 h for the H_2PtCl_6 concentrations used in this experiment) and the other much longer than it. Clearly, the adsorption/desorption currents increased with the H_2PtCl_6 concentration and were independent of t_{SD}. This means that, once all the Pt had deposited onto the Ni foam, the Pt surface area remained unchanged upon prolonging the immersion. Fig. 4 also shows that the adsorption/desorption currents measured with different electrodes treated in solutions with the same H_2PtCl_6 concentration, were very close to each other. It may be concluded that exhaustive deposition of Pt onto Ni foams reproducibly yielded modified electrodes, with well-defined Pt surface areas, which were stable in the depleted spontaneous deposition media.

The cyclic voltammograms in Fig. 5, obtained with Ni foam samples modified with variable Pt amounts, showed a regular increase in the hydrogen adsorption/desorption currents for increasing Pt loadings. Furthermore, the charges associated to the $Ni(OH)_2/NiOOH$ redox system underwent a slight increase, with respect to an etched foam, when Pt loading was 8.1 mg cm^{-2}, and the increase became progressively stronger at higher concentrations. Such a trend shows that the oxidation of the foam material by $Pt^{4þ}$ caused a roughening of the Ni substrate and an increase in its surface area, as already observed for several other systems [7,23,33,36].

A similar investigation, carried out with electrodeposited porous Ni layers, showed rather good reproducibility when t_{SD} was well below t_{SD}^{o}, but led to scattered and unsatisfactory results when t_{SD}^{o} was approached or exceeded, most probably because of the extensive corrosion of Ni highlighted by SEM (Fig. 1B). The cyclic voltammograms shown in Fig. 6 were obtained with electrodeposited Ni porous layers modified with variable Pt amounts, in an extended potential range. The hydrogen adsorption/desorption region is highlighted in the inset. The intensity of the peaks associated to hydrogen adsorption/desorption markedly increased with the Pt loading. Those of the peaks due to the $Ni(OH)_2/NiOOH$ also increased, though in a much less pronounced way. Therefore, it is clear that both kinds of Ni substrate behaved similarly. However, a comparison of Figs. 5 and 6 makes immediately clear that, for comparable Pt loadings, the surface areas of the Pt deposits on the foams were significantly higher than those on the

porous layers.

3.3. Pt loading and Pt surface area of modified electrodes

The hydrogen desorption charges were systematically measured with Pt-modified Ni electrodes with variable loadings, and divided by the desorption charge (per cm^2) measured with a carefully polished Pt disc electrode, under the same conditions (solution, scan rate, E_A), to obtain the respective Pt surface areas, henceforth denoted A_{Pt}, reported in Table 1. The dependence of the ratio A_{Pt}/A_{Ni}, where A_{Ni} is the surface area of the Ni substrate, on the Pt loading per unit true Ni surface area, L^S_{Pt}, is reported in Fig. 7A. For both Ni substrates the ratio A_{Pt}/A_{Ni} increased with L^S_{Pt} in a roughly linear way and, at each loading was significantly higher for the foam than for the porous layers. Foam samples with $L^S_{Pt} > 30$ mg cm^{-2} had A_{Pt}/A_{Ni} ratios larger than 1; i.e. the area of the Pt deposits exceeded that of the Ni substrate; in the case of porous Ni electrodeposits, such a result was achieved only with ca. 4 times higher $_{Pt}$ values. Surface area and loading data were used to calculate the values of Pt surface area per unit Pt mass reported in Fig. 7B. An average value around 3 $m^2\ g^{-1}$, was obtained for foam electrodes, whereas the values for porous electrodeposits were mostly below 1 $m^2\ g^{-1}$. The former value, little dependent on loading in the explored range, was somewhat lower but of the same order of that measured with Pd-modified Ni foam electrodes [23], and ca. 4 times lower than that reported by Yamauchi et al. [15] for Pt particles spontaneously deposited onto Ni foams from lyotropic liquids.

3.4. Hydrogen evolution reaction

Polarization curves were recorded, in 1 M KOH, with Pt- modified porous Ni electrodeposits (A) and Pt-modified Ni foams (B) with variable loading. Fig. 8 shows Tafel plots obtained in the HER potential range (potential was corrected for ohmic drop). In each part of the figure, the bottom scale reports the current density j referred to the true surface area of the Ni substrates, while the top scale reports j_{geo}, i.e. the current density referred to the geometric area of the electrodes. The ratios between the top and bottom scales are identical to the ratios between true and geometric surface areas, and therefore correspond to the surface

roughness factors of each Ni substrate (ca. 20 for the electrodeposits, ca. 16 for foam electrodes).

Both sets of curves in Fig. 8 show that the HER was very significantly catalyzed even with the lowest loadings tested (L^{S}_{Pt} < 5 mg cm^{-2}). The activity of the electrodes progressively increased upon increasing L^{S}_{Pt}, but the gain in activity became less significant at L^{S}_{Pt} > 50 mg cm^{-2} for porous electrodeposits and at L^{S}_{Pt} > 30 mg cm^{-2} for foams. The Tafel slopes varied between 113 and 146 mV for Pt-modified porous Ni electrodeposits and between 114 and 159 mV for Pt-modified Ni foams, with no well-defined dependence on Pt loading in either case. These Tafel slope values are in essential agreement with those, close to 120 mV, reported in classical studies on the HER at Pt electrodes in alkaline media [42e44], which suggested either the hydrogen adsorption, at low coverage, or the electrochemical desorption in parallel with recombination, at high coverage, to be the rate determining steps.

A parameter often employed to compare the activity of different electrodes in the HER is the overpotential necessary to cause a fixed current density, normally referred to the geometric area. In Fig. 9, h_{100}, defined as the overpotential at which j_{geo} ¼ -100 mA cm^{-2}, is plotted as a function of the Pt loading L^{S}_{Pt}. The h_{100} values decreased as L^{S}_{Pt} increased, were generally lower for foam electrodes than for porous electro- deposits but, for both kinds of Ni substrates, approached a common limiting value around -75 mV. It is interesting to compare such a value with those reported in the literature and obtained under comparable conditions (1 M NaOH or KOH, at room temperature) with other electrode materials. For cath- odes based on non-noble metals only, h_{100} usually exceeded 200 mV (see, for example [1,45e50],). For cathodes containing noble metals, Fournier et al. [51] measured h_{100} between -56 and - 104 mV with Pt-graphite-$LaPO_4$ electrodes, Spataru et al. [52] found h_{100} to be ca. -120 mV for thin film RuO_2 electrodes, and Dumont et al. [24,53] reported h_{250} and Tafel slopes corresponding to h_{100} of -42 to -43 mV for $LaPO_4$-bonded Ni-Rh [53] and Ni-Ru [24] cathodes. Therefore, the results described in the present paper are fully comparable, in terms of h_{100}, with those obtained with active noble metal-based electrodes described in the literature which, however, were often prepared through complicated synthetic routes and had higher noble metal loadings (see below).

Similar information is obtained by plotting the dependence on L^S_{Pt} of the current density (referred to the true Ni support surface area) measured at an overpotential h ¼ -100 mV, henceforth denoted j_{100}, Fig.10A. This figure shows that j_{100} increased with L^S_{Pt} and that, at each loading, the foam electrodes were more active than the electrodeposits. However, when the total current measured at an over- potential h ¼ -100 mV, denoted i_{100}, was plotted as a function of the Pt surface area (Fig. 10B), the performance of both kinds of electrodes became closer. Thus, it may be concluded that the higher activity of the foam electrodes, highlighted by Fig. 10A, was mainly due to their higher Pt surface area per unit Pt mass (as shown in Fig. 7B). The residual differences shown by Fig. 10B may be possibly ascribed to the easier release of hydrogen bubbles from the relatively larger pores of the foams, as compared to the Ni electrodeposits.

As the cost of the electrodes, which has a major impact on their application potential, depends mainly on their Pt loading, this parameter cannot be neglected when their activity is discussed. Fig. 11 shows the mass activity of the electrodes (conventionally defined as the ratio between j_{100} and L^S_{Pt}) plotted as a function of L^S_{Pt}. The mass activity of the foam electrodes, always higher than that of the porous electrodeposits with the same loading, was higher than 700 A g^{-1} at low loading and progressively decreased to 150-200 A g^{-1} for increasing L^S_{Pt} values. Comparison with data in the literature is difficult because the noble metal loading is not always explicitly reported. However, one can calculate a mass activity of 25 A g-1 for thin film RuO2 electrodes [52], and estimate mass activities of the order of 10 A g-1 for LaPO4-bonded cathodes containing Pt, Rh or Ru [24,51,53]. Although the mass activity of the latter systems was clearly not optimized, this comparison underlines the potential interest of the electrodes described in the present work.

4. Conclusions

The spontaneous deposition of Pt on Ni substrates with large surface areas, and the HER at the Pt-modified electrodes thus obtained were studied. Pt deposits were effectively obtained on both Ni porous electrodeposits and commercial Ni foams, with procedures similar to those employed, for various noble metals, in previous investigations, e.g. [5-7, 15, 23, 33, 36]. Nevertheless, there were significant differences between the two substrates, in terms of (i) the most effective deposition procedure, (ii) the Pt particle distribution and (iii) their surface area to mass ratio.

- The exhaustive deposition of Pt, i.e. the deposition of all the noble metal contained in small volumes of diluted H_2PtCl_6 solutions, was an easy way to control the Pt loading of the foam electrodes which were quite resistant to corrosion in the plating solutions. However, implying fairly long reaction times, such an approach caused significant corrosion of the Ni electrodeposits for which milder procedures had to be adopted.

- Possibly due to mass transfer limitations within the narrow pores of the Ni electrodeposits, Pt nuclei were unevenly distributed on their surface, due to a preferential growth on the top of the Ni dendrites constituting the deposits. Such limitations were unimportant for the Ni foams and so the walls of both their inner and outer cells were coated by comparable deposits.

- At comparable loadings, the true Pt surface area was significantly higher for the foams than for the electrode- posits, but not as high as reported in other spontaneous deposition studies [15,23].

A strong catalysis of HER in basic solutions was detected already with Pt loadings as low as 5 mg cm^{-2}; then, the electrode activity progressively increased by increasing the loading, to approach a limiting value. Foam electrodes were significantly more active than electrodeposits at low loading, where their mass activities were high, but the differences diminished with increasing loadings. Thus, the lowest overpotential necessary to cause a -100 mA cm^{-2} HER current density (referred to geometric area) was around -75 mV for both Ni large-area substrates. This value is fully comparable with those measured with active noble

metal-based electrodes described in the literature [24, 51-53] which, however, had markedly lower mass activity (referred to the respective noble metals) than the Pt-modified Ni foam electrodes described in this work.

Acknowledgments

The authors from IENI-CNR acknowledge the financial support of the Italian Ministry for Economic Development (MSE) e MSE-CNR Agreement on National Electrical System. I. Herraiz-Cardona is grateful to the *Ministerio de Educación* of Spain for a post-graduate grant (Ref. AP2007-03737). The authors are indebted to Dr. Arianna Gambirasi, ICIS CNR, Padova, Italy for recording SEM images and to FILA INDUSTRIA CHIMICA SPA, San Martino di Lupari, Padova, Italy, owner of the Fei-ESem FEI Quanta 200 FEG instrument, for allowing its use for the research work described in this article.

References.

[1] Bockris JO. A hydrogen economy. In: Bockris JO, Conway BE, Yeager E, White RE, editors. Comprehensive treatise of electrochemistry, vol. 3. New York: Plenum; 1981. p. 505-26.

[2] Veziroglu TN, Barbir F. Hydrogen e the wonder fuel. Int J Hydrogen Energy 1992;17:391-404.

[3] Trasatti S. Electrocatalysis of hydrogen evolution: progress in cathode activation. In: Gerischer H, Tobias CW, editors. Advances in electrochemical science and engineering, vol. 2. Weinheim: VCH; 1992. p. 1.

[4] Pletcher D, Li X. Prospects for alkaline zero gap water electrolysers for hydrogen production. Int J Hydrogen Energy 2011;36:15089-104.

[5] Grove DE. Precious-metal activated cathodes for chloralkali cells. In: Wall K, editor. Modern chlor-alkali technology, vol. 3. Horwood: SCI; 1986. p. 250-62.

[6] Cameron DS, Phillips RL, Willis PM. Poison tolerant platinum catalysed cathodes for membrane cells. In: Prout NM, Moorhouse JS, editors. Modern chlor-alkali technology, vol. 4. SCI/Elsevier Applied Science; 1990. p. 95-107.

[7] Vázquez-Gómez L, Cattarin S, Guerriero P, Musiani M. Hydrogen evolution on porous Ni cathodes modified by spontaneous deposition of Ru or Ir. Electrochim Acta 2008;53:8310-8.

[8] Vázquez-Gómez L, Cattarin S, Gerbasi M, Guerriero P, Musiani M. Activation of porous Ni cathodes towardshydrogen evolution by electrodeposition of Ir nuclei. J Appl Electrochem 2009;39:2165-72.

[9] Marozzi CA, Chialvo AC. Development of electrode morphologies of interest in electrocatalysis. Part 1: electrodeposited porous nickel electrodes. Electrochim Acta 2000;45:2111-20.

[10] Marozzi CA, Chialvo AC. Development of electrode morphologies of interest in electrocatalysis: part 2: hydrogen evolution reaction on macroporous nickel electrodes. Electrochim Acta 2001;46:861-6.

[11] Huet F, Musiani M, Nogueira RP. Oxygen evolution on electrodes of different roughness: an electrochemical noise study. J Solid State Electrochem 2004;8:786-93.

[12] Skowronski JM, Wazny A. Nickel foam-based composite electrodes for electrooxidation of methanol. J Solid State Electrochem 2005;9:890-9.

[13] Yang W, Yang S, Sun W, Sun G, Xin Q. Nanostructured silver catalyzed nickel foam cathode for an aluminumehydrogen peroxide fuel cell. J Power Sources 2006;160:1420-4.

[14] Yang W, Yang S, Sun W, Sun G, Xin Q. Nanostructured palladiumesilver coated nickel foam cathode for magnesiumehydrogen peroxide fuel cells. Electrochim Acta 2006;52:9-14.

[15] Yamauchi Y, Kumatsu M, Takai A, Sebata R, Sawada M, Momma T, et al. Direct deposition of nanostructured Pt particles onto a Ni foam from lyotropic liquid crystalline phase by displacement plating. Electrochim Acta 2007;53:604-9.

[16] Bidault F, Brett DJL, Middleton PH, Abson N, Brandon NP. A new application for nickel foam in alkaline fuel cells. Int J Hydrogen Energy 2009;34:6799-808.

[17] Bidault F, Brett DJL, Middleton PH, Abson N, Brandon NP. An improved cathode for alkaline fuel cells. Int J Hydrogen Energy 2010;35:1783-8.

[18] Cao D, Guo Y, Wang G, Miao R, Liu Y. A direct NaBH4eH2O2 fuel cell using Ni foam supported Au nanoparticles as electrodes. Int J Hydrogen Energy 2010;35:807-13.

[19] Wang YL, Zhao YQ, Xu CL, Zhao DD, Xu MW, Su ZX, et al. Improved performance of Pd electrocatalyst supported on three-dimensional nickel foam for direct ethanol fuel cells. J Power Sources 2010;195:6496-9.

[20] Cheng Y, Liu Y, Cao D, Wang G, Gao Y. Effects of acetone on electrooxidation of 2-propanol in alkaline medium on the Pd/ Ni-foam electrode. J Power Sources 2011;196:3124-8.

[21] He H, Liu H, Liu F, Zhou K. Structures and electrochemical properties of amorphous nickel sulphur coatings electrodeposited on the nickel foam substrate as hydrogen evolution reaction cathodes. Surf Coat Technol 2006;201: 958-64.

[22] Yang B, Yu G, Shuai D. Electrocatalytic hydrodechlorination of 4-chlorobiphenyl in aqueous solution using palladized nickel foam cathode. Chemosphere 2007;67:1361-7.

[23] Verlato E, Cattarin S, Comisso N, Gambirasi A, Musiani M, Vá zquez-Gó mez L. Preparation of Pd-modified Ni foam electrodes and their use as anodes for the oxidation of alcohols in basic media. Electrocatalysis 2012;3:48-58.

[24] Dumont H, Los P, Lasia A, Mé nard H. Studies of the hydrogen evolution reaction on lanthanum phosphate-bonded composite nickeleruthenium electrodes in 1 M alkaline solutions. J Appl Electrochem 1993;23:684-92.

[25] Brankovic SR, Wang JX, Adžić RR. Metal monolayer deposition by replacement of metal adlayers on electrode surfaces. Surf Sci 2001;474:L173-9.

[26] Sasaki K, Mo Y, Wang JX, Balasubramanian M, Uribe F, McBreen J, et al. Pt submonolayers on metal nanoparticles-novel electrocatalysts for H2 oxidation and O2 reduction. Electrochim Acta 2003;48:3841-9.

[27] Zhang J, Mo Y, Vukmirovic MB, Klie R, Sasaki K, Adžić RR. Platinum monolayer electrocatalysts for O_2 reduction: Pt monolayer on Pd(111) and on carbon-supported Pd nanoparticles. J Phys Chem B 2004;108:10955-64.

[28] Bianchi I, Guerrini E, Trasatti S. Electrocatalytic activation of Ni for H_2 evolution by spontaneous deposition of Ru. Chem Phys 2005;319:192-9.

[29] Papadimitriou S, Tegou A, Pavlidou E, Kokkinidis G, Sotiropoulos S. Methanol oxidation at platinized lead coatings prepared by a two-step electrodeposition-electroless deposition process on glassy carbon and platinum substrates. Electrochim Acta 2007;52: 6254-60.

[30] Papadimitriou S, Tegou A, Pavlidou E, Armyanov S, Valova E, Kokkinidis G, et al. Preparation and characterisation of platinum- and gold-coated copper, iron cobalt and nickel deposits on glassy carbon substrates. Electrochim Acta 2008; 53:6559-67.

[31] Ghodbane O, Roué L, Bélanger D. Study of the electroless deposition of Pd on Cu-modified graphite electrodes by metal exchange reactions. Chem Mater 2008;20:3495-504.

[32] Tegou A, Armyanov S, Valova E, Steenhaut O, Hubin A, Kokkinidis G, et al. Mixed platinumegold electrocatalysts for borohydride oxidation prepared by the galvanic replacement of nickel deposits. J Electroanal Chem 2009;634:104-10.

[33] Verlato E, Cattarin S, Comisso N, Guerriero P, Musiani M, Vázquez-Gómez L. Preparation of catalytic anodes for methanol oxidation by spontaneous deposition of Pd onto porous Ni or porous Co. Electrochem Commun 2010;12: 1120-3.

[34] Podlovchenko BI, Gladysheva TD, Filatov AY, Yashina LV. The use of galvanic displacement in synthesizing Pt(Cu) catalysts with the core-shell structure. Russ JElectrochem 2010;46:1189-97.

[35] Tveritinova EA, Maksimov YM, Zhitnev YN, Podlovchenko BI, Lunin VV. Use of galvanic displacement in the synthesis of a Pd(Cu) hydrodechlorination catalyst. Mendeleev Commun 2010;20:10-1.

[36] Vázquez-Gómez L, Verlato E, Cattarin S, Comisso N, Guerriero P, Musiani M. Electrodeposition of porous Co layers and their conversion to electrocatalysts for methanol oxidation by spontaneous deposition of Pd. Electrochim Acta 2011;56:2237-45.

[37] Sattar MA, Conway BE. Electrochemistry of the nickel-oxide electrodeeVI. Surface oxidation of nickel anodes in alkaline solution. Electrochim Acta 1969;14:695-710.

[38] Woods R. Chemisorption at electrodes: hydrogen and oxygen on noble metals and their Alloys. In: Bard AJ, editor. Electroanalytical chemistry, vol. 9. New York: Marcel Dekker; 1976. p. 1.

[39] Woods R. Hydrogen adsorption on platinum, iridium and rhodium electrodes at reduced temperatures and the determination of real surface area. J Electroanal Chem 1974; 49:217-26.

[40] Visintin A, Triaca WE, Arvia AJ. Changes in the surface morphology of platinum electrodes produced by the application of periodic potential treatments in alkaline solution. J Electronal Chem 1990;284:465-80.

[41] Marinkovic NS, Markovic NM, Adzic RR. Hydrogen adsorption on single-crystal platinum electrodes in alkaline solutions. J Electroanal Chem 1992;330:433-52.

[42] Ammar IA, Darwish S. Overpotential on activated platinum cathodes in sodium hydroxide solutions. J Phys Chem 1959; 63:983e5.

[43] Bockris JOM, Srinivasan S. Elucidation of the mechanism of electrolytic hydrogen evolution by the use of H-T separation factors. Electrochim Acta 1964;9:31-44.

[44] Conway BE, Bai L. Determination of adsorption of OPD H species in the cathodic hydrogen evolution reaction at Pt in relation to electrocatalysis. J Electroanal Chem 1986;198: 149-75.

[45] Lasia A. Hydrogen evolution reaction. In: Vielstich W, Gasteiger HA, Lamm A, editors. Handbook of fuel cells e fundamentals, technology and applications, vol. 2. Johnn Wiley & Sons, Ltd; 2003. p. 416-40.

[46] Simpraga R, Tremiliosi-Filho G, Quian SY, Conway BE. In situ determination of the real area factor in H_2 evolution electrocatalysis at porous NieFe composite electrodes. J Electroanal Chem 1997;424:141-51.

[47] Shervedani RK, Lasia A. Studies of the hydrogen evolution reaction on NieP electrodes. J Electrochem Soc 1997;144: 511-9.

[48] Shervedani RK, Lasia A. Study of the hydrogen evolution reaction on NieMoeP electrodes in alkaline solutions. J Electrochem Soc 1998;145:2219 25.

[49] Jakšić JM, Vojnović MV, Krstajić. Kinetic analysis of hydrogen evolution at NieMo alloy electrodes. Electrochim Acta 2000; 45:4151-8.

[50] Bocutti R, Saeki MJ, Florentino AO, Oliveira CLF, Â ngelo ACD. The hydrogen evolution reaction on codeposited Ni-hydrogen storage intermetallic particles in alkaline medium. Int J Hydrogen Energy 2000;25:1051-8.

[51] Fournier J, Brossard L, Tilquin JY, Cô té R, Dodelet JP, Guay D, et al. Hydrogen evolution reaction in alkaline solution e catalytic influence of Pt supported on graphite vs. Pt inclusion in graphite. J Electrochem Soc 1996;143:919-26.

[52] Spa taru N, Le Holloco JG, Durand R. A study of RuO2 as an electrocatalyst for hydrogen evolution in alkaline solution. J Appl Electrochem 1996;26:397-402.

[53] Dumont H, Los P, Brossard L, Lasia A, Mé nard H. Lanthanum phosphate-bonded composite nickelerodhium electrodes for alkaline water electrolysis. J Electrochem Soc 1992;139:2143-8

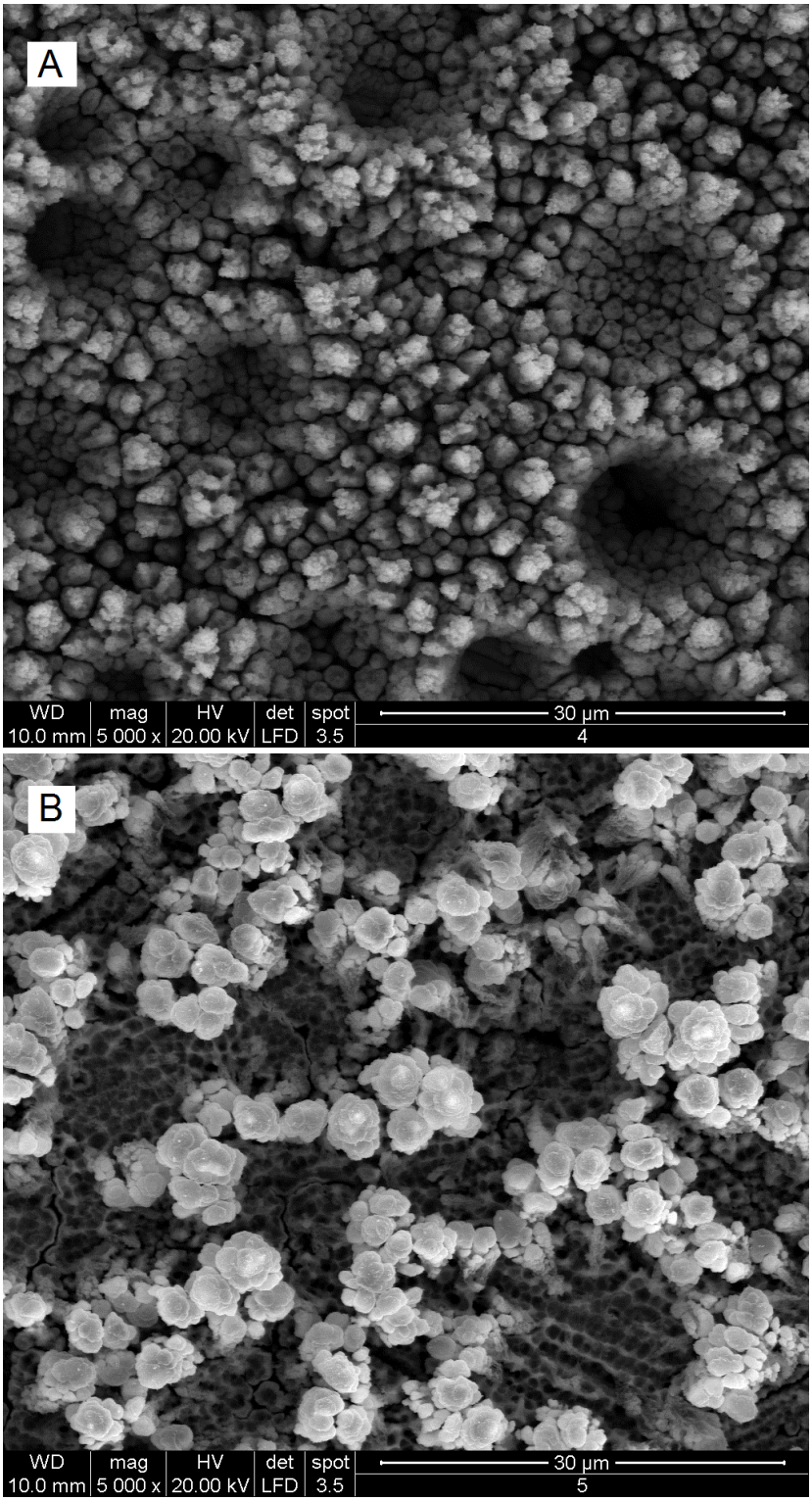

Fig. 1. SEM images of porous Ni electrodeposits immersion plated in 30 mL of 6.8 $\cdot 10^{-5}$ M H_2PtCl_6 solution for 8 hours (A) and in 30 mL of 1.37 $\cdot 10^{-4}$ M H_2PtCl_6 solution for 16 hours (B).

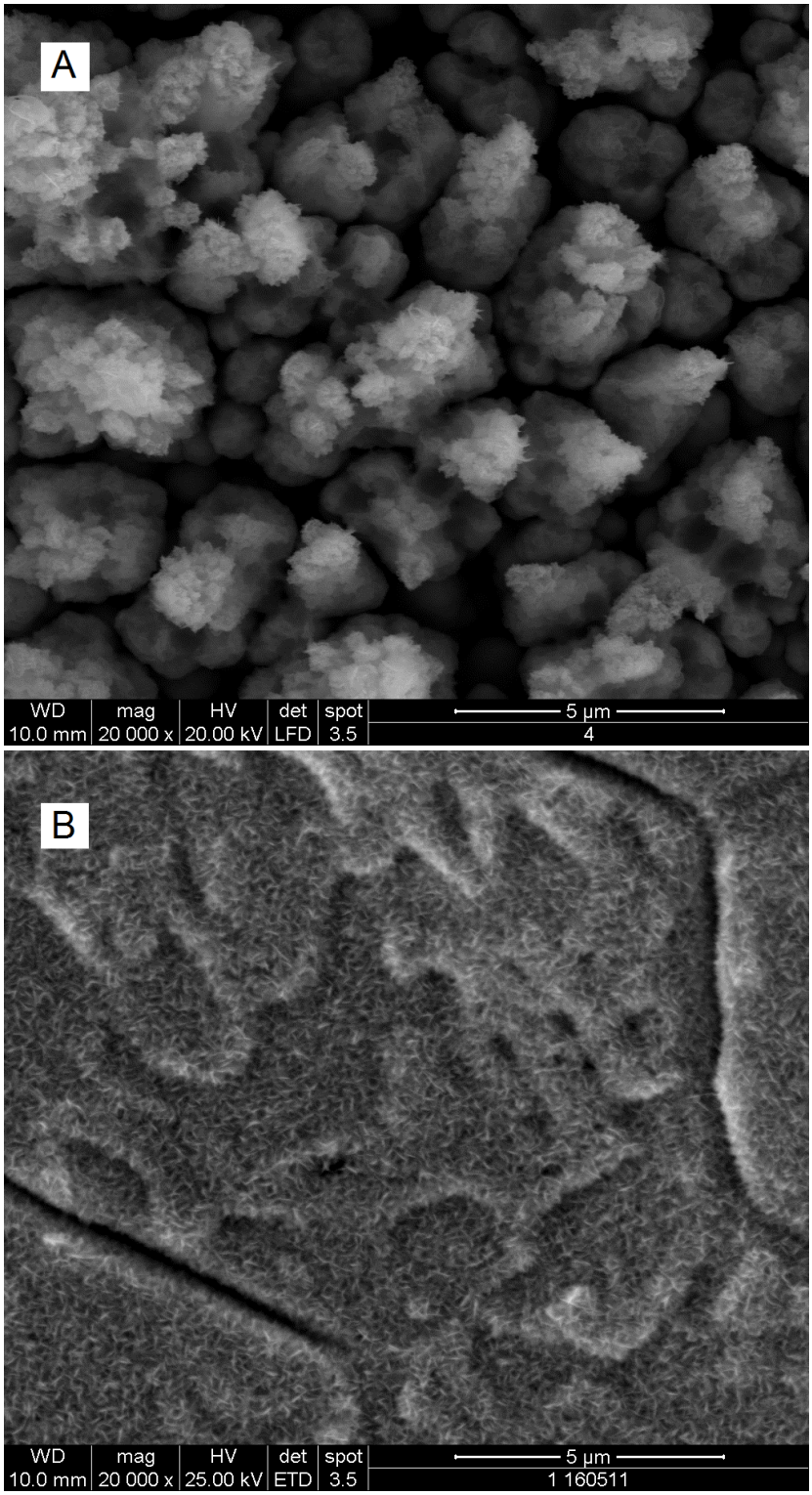

Fig. 2. SEM images of a Pt-modified porous Ni electrodeposit with L^{s}_{Pt} = 49.5 µg cm^{-2} (A) and of a Pt-modified Ni foam with L^{s}_{Pt} = 83 µg cm^{-2} (B). Loadings are referred to the true surface area of the Ni substrates.

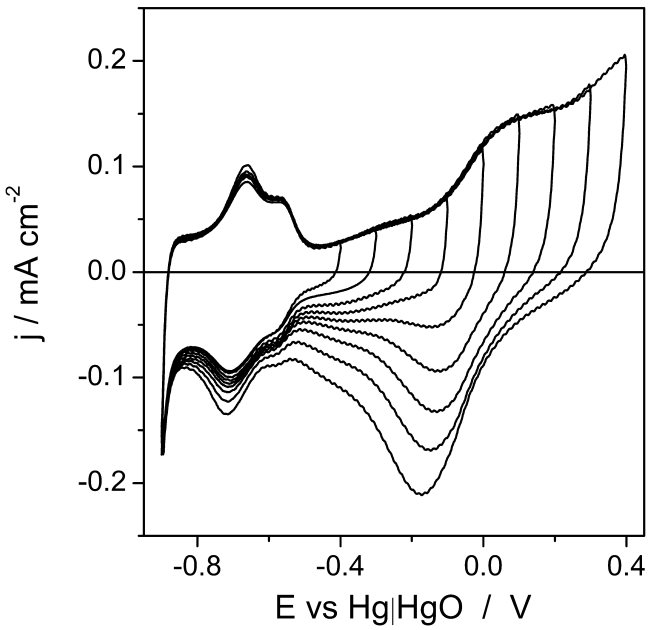

Fig. 3. Cyclic voltammograms recorded with a Pt disc electrode in 1 M KOH, at 50 mV s^{-1} and variable anodic limit.

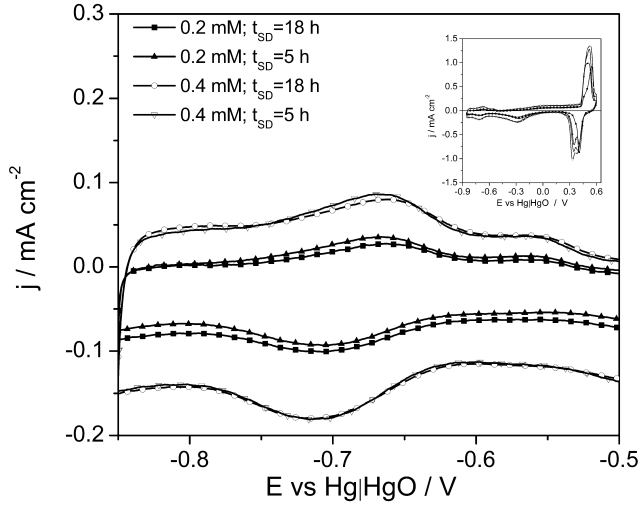

Fig. 4. Cyclic voltammograms recorded with Pt-modified Ni foam electrodes in 1 M KOH, at 50 mV s^{-1}, in the hydrogen adsorption/desorption region. Spontaneous deposition conditions are reported on the figure. The inset shows the same voltammograms in a wider potential range encompassing the $Ni(OH)_2$/NiOOH system.

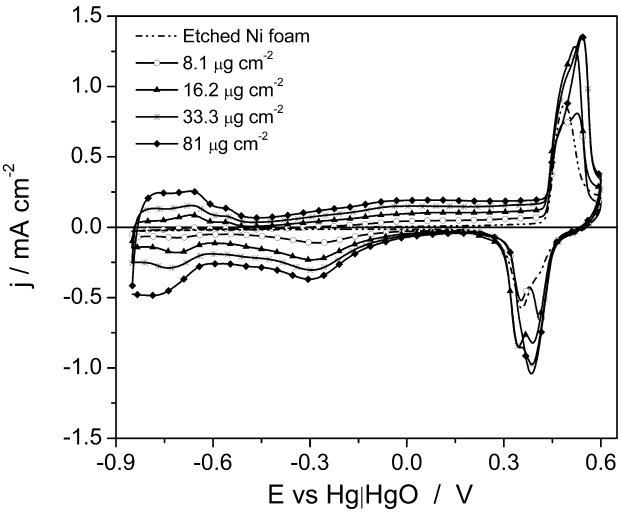

Fig. 5. Cyclic voltammograms recorded with a Ni foam electrode and four Pt-modified Ni foam electrodes with variable loading, indicated on the figure, in 1 M KOH, at 50 mV s^{-1}.

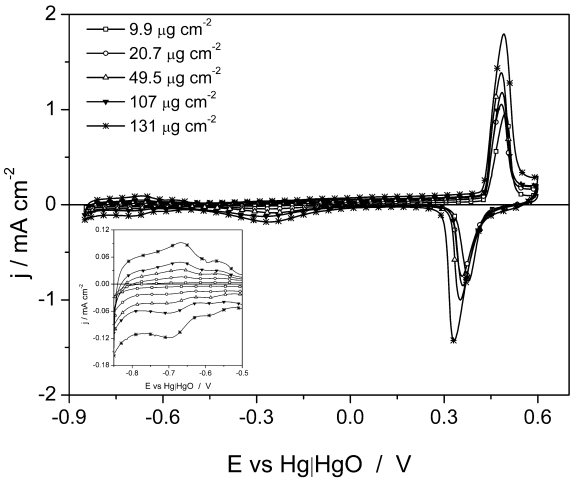

Fig 6. Cyclic voltammograms recorded with Pt-modified porous Ni electrodeposits with variable loading, indicated on the figure, in 1 M KOH, at 50 mV s^{-1}.

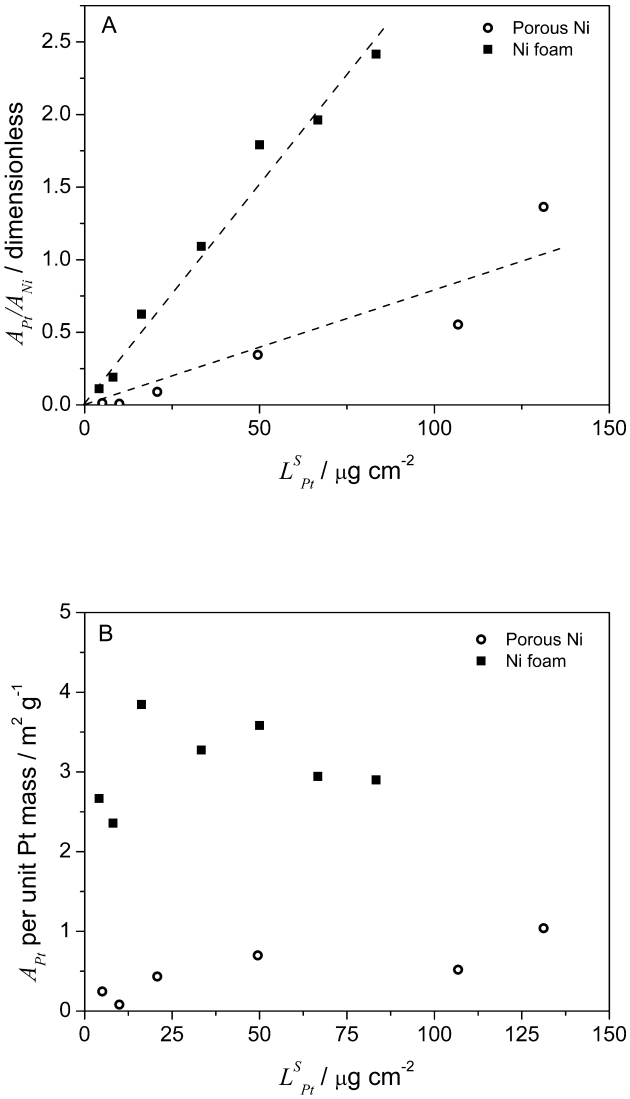

Fig. 7. Dependence of the true surface area of Pt deposits, normalized with respect to the surface area of the Ni substrate (A) and of the Pt surface area per unit Pt mass (B) on the loading of Ptmodified Ni electrodes. The dashed lines are just an aid for the eye.

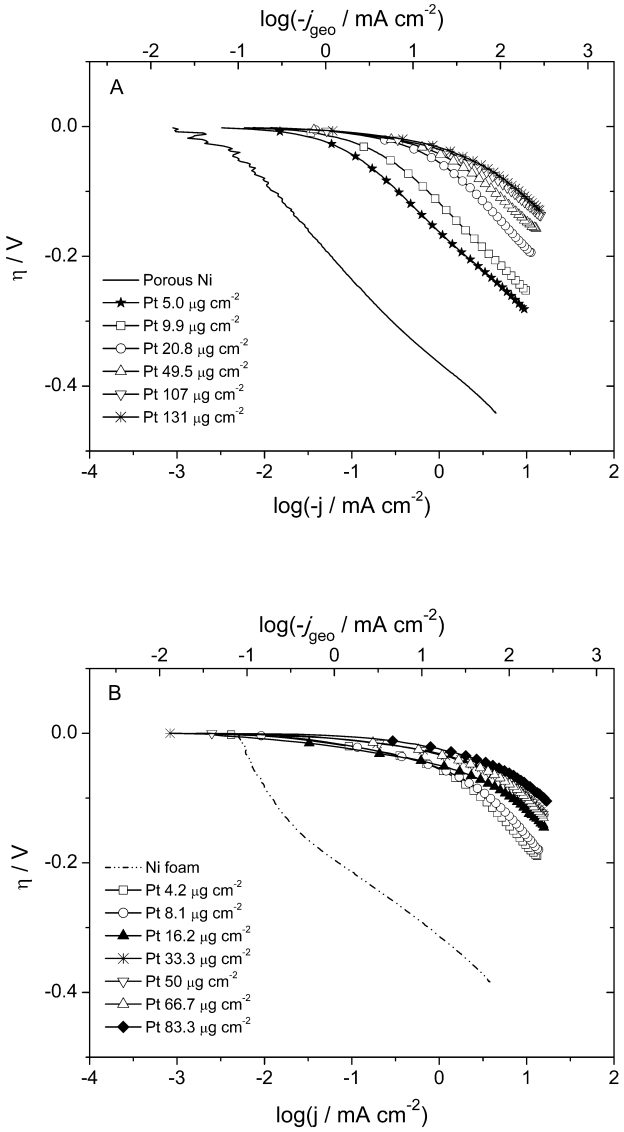

Fig. 8. Polarization curves recorded with Pt-modified porous Ni electrodeposits (A) and Pt-modified Ni foams (B) in 1 M KOH, at 50 mV s^{-1}. The Pt loading per unit surface area of the Ni supports is indicated on the figures.

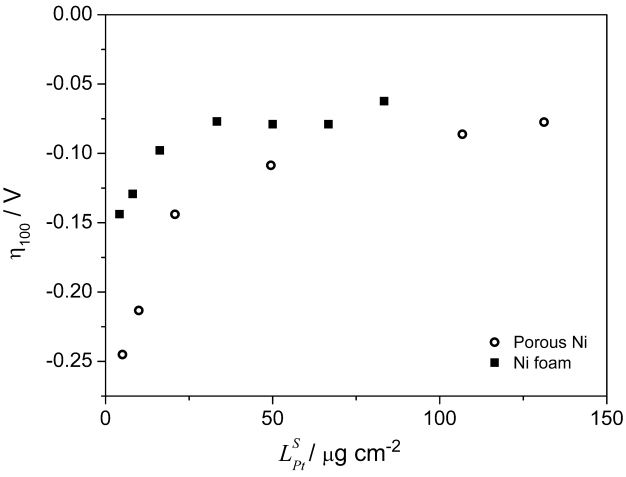

Fig. 9. Dependence of the overpotential for the HER, measured at a current density j_{geo} = -100 mA cm^{-2}, on the Pt loading of the electrodes

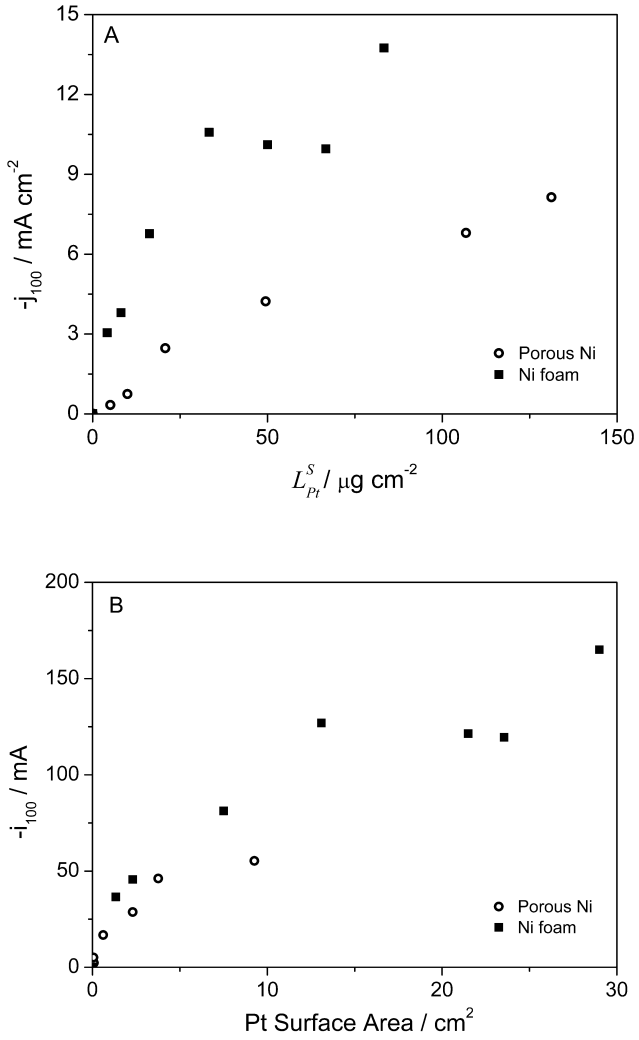

Fig. 10. A: Dependence of the current density for HER, measured at η = -100 mV, on the Pt loading; B: Dependence of the current for HER, measured at η = -100 mV, on the Pt surface area.

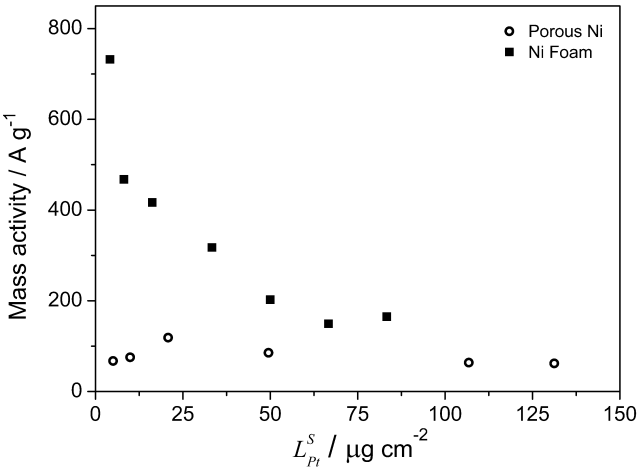

Fig. 11. Dependence of the mass activity, defined as j_{100} / L^{s}_{Pt} of modified Ni electrodes, for HER in 1 M KOH, on the Pt loading.